AD-A189 324 THE EFFECTS OF ATMOSPHERIC AND THERMOHALINE VARIABILITY ON THE VALIDATION..(U) SACLANT ASW RESEARCH CENTRE LA SPEZIA (ITALY) P J MINNETT OCT 87 SACLANTCEN-SR-128 1/1

UNCLASSIFIED F/G 8/3 NL

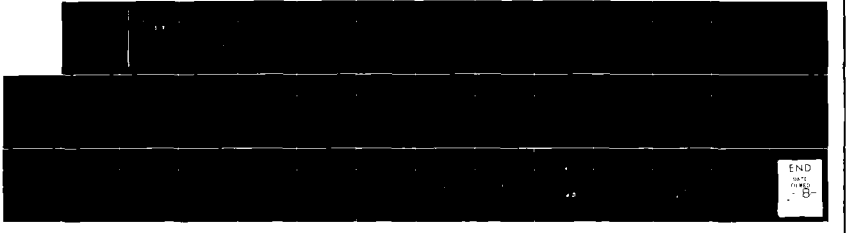

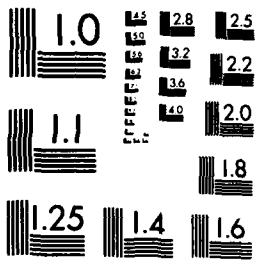

(4)

DTIC FILE COPY

AD-A189 324

SACLANTCEN REPORT
serial no.: SR-128

SACLANT ASW
RESEARCH CENTRE
REPORT

DTIC
ELECTE
DEC 1 1 1987
S D
H

The effects of atmospheric and thermohaline variability on the validation of the GEOSAT altimeter oceanographic signal between Scotland and Iceland

P.J. Minnett

October 1987

The SACLANT ASW Research Centre provides the Supreme Allied Commander Atlantic (SACLANT) with scientific and technical assistance under the terms of its NATO charter, which entered into force on 1 February 1963. Without prejudice to this main task—and under the policy direction of SACLANT—the Centre also renders scientific and technical assistance to the individual NATO nations.

87 12 1 0

SACLANTCEN SR-128

The effects of atmospheric and thermohaline variability on the validation of the GEOSAT altimeter oceanographic signal between Scotland and Iceland

P.J. Minnett

The content of this document pertains to work performed under Project 23 of the SACLANTCEN Programme of Work. The document has been approved for release by The Director, SACLANTCEN.

Ralph R. Goodman
Director

intentionally blank page

The effects of atmospheric and thermohaline variability on the validation of the GEOSAT altimeter oceanographic signal between Scotland and Iceland

P.J. Minnett

Abstract: Atmospheric and oceanographic profiles from the area between Scotland and Iceland are analysed in order to predict the magnitudes of the errors they can induce in satellite altimeter measurements of sea-surface topography. This is the area where the second phase of the COMPASS project will take place in early 1988, and the aim is to provide absolute calibration data for the GEOSAT altimeter by using coastal land-based active microwave transponders. While most of the variability in the sea-surface topography can be ascribed to variations in the temperature profile, the spatial changes in the temperature-salinity relationship are such that errors in the sea-surface topography predicted from measured temperature profiles can not be neglected. This means that the validation of the altimeter oceanographic signal can not be done in this area by using only the more readily-available temperature profiles from expendable probes. The atmospheric variability characteristic of this area can induce errors in the altimeter range measurement comparable to the oceanographic signal, and careful corrections are necessary. These will have to faithfully reflect the changes in atmospheric properties along the COMPASS arc.

Keywords: atmospheric variability ○ AXBT ○ COMPASS ○ GEOSAT ○ GIN86 ○ satellite altimeter ○ sea-surface topography ○ thermohaline variability ○ TOPEX-Poseidon ○ XBT

Contents

1. Introduction

The earth's geoid is the sea-level gravitational equipotential surface and this shape would be assumed by the sea-surface in the absence of ocean currents. The shape of the geoid is determined by the internal mass distribution in the earth and by the acceleration of the earth's rotation. The departure of the ocean surface from the geoid, the sea-surface topography, can be related to the near-surface geostrophic currents. The undulations in the sea-surface topography can be in excess of 1 m at the fronts associated with Western Boundary Currents (Gulf Stream and Kuroshio), but are generally less elsewhere (see Table 1). In principle, radar altimeters on earth-satellites in near-polar orbits can provide measurements of the surface topography on a global scale and with adequate accuracy. The demonstrated precision of satellite altimeter range measurements is currently about 10 cm, with the prospect of reduction to $\sim$ 2 cm in future altimetric satellite missions such as TOPEX-Poseidon (Born, Wunsch and Yamarone, 1984).

1.1. UNCERTAINTIES IN ALTIMETER RANGE MEASUREMENTS

While a measurement of ocean topography to decimetre precision is technically feasible, there are many sources of uncertainty which are difficult to remove to the same accuracy (Fig. 1). In particular, the geoid itself is not known with sufficient accuracy and spatial resolution in many parts of the world ocean. However, since the geoid is constant on the timescales of interest, the differences between altimeter measurements over the same section from orbits repeated after intervals of days to weeks can reveal changes in the ocean currents. Thus an estimate of the current variability can be made even when the measurement of the absolute current itself is unattainable.

Other sources of uncertainty in the absolute range measurements of satellite altimeters are:

(a) in the position of the satellite in space, i.e. in the determination of the orbit;

(b) in the changes in the refractive index of the media between the satellite and the sea-surface caused by variations in the free electron content of the ionosphere, changes in the mass of the atmosphere, and variability of the water vapour content of the troposphere;

(c) in the variability of the shape of the sea-surface caused by unresolved surface waves within the altimeter field of view, which is typically several kilometres in diameter. This is called the sea-state bias or the electromagnetic bias, and is a function of the surface wave field;

(d) tides which can produce time-varying signals in the sea-surface topography comparable to the geostrophic signals.

It is generally the case that residual instrumental effects produce smaller uncertainties than those from the above sources, provided that the altimeter tracking circuits are locked-on to the sea-surface echo; otherwise no useful signal is obtained.

TABLE 1
Typical oceanic topography signals (from Stewart, 1985)

Phenomenon	Typical surface expression	Period of variability	Comments
Western boundary currents (Gulf Stream, Kuroshio)	130 cm/100 km	days to years	variability in position and 25% variability in transport
Large gyres	50 cm/3000 km	one to many years	25% variability expected
Eastern boundary currents	30 cm/100 km	days to years	100% variability expected, maybe reversals of direction
Mesoscale eddies	25 cm/100 km	about 100 days	100% variability
Rings	100 cm/100 km	weeks to years	100% variability
Equatorial currents	30 cm/5000 km	months to years	100% variability
Tides	100 cm/5000 km	hours to years	aliased to low frequency

1.2. IN-SITU VALIDATION OF THE ALTIMETER TOPOGRAPHY

Even after all the available corrections have been applied to the altimeter measurement, there will remain residual uncertainties. The most satisfactory way of ensuring that these are sufficiently small is to compare the altimetric sea-surface topography with that derived from coincident conventional hydrographic data. The most suitable in-situ data are from precision pressure sensors mounted on the sea-bottom and from high-quality oceanographic profiles through the water column.

The number of available pressure sensors is small, and they tend to be deployed at fixed locations over a period of time. Profiles, on the other hand, are not restricted to specific locations, but their total number is limited by available aircraft or ship time. At best the profile data are of specific volume anomaly, which have been derived from high-quality, calibrated profiles produced by instruments (CTDs) measuring electrical conductivity, temperature and depth. These measurements are integrated with respect to depth to give the dynamic height anomaly of the water column. In reality, such profiles are time-consuming to gather and require considerable ship time. Thus even a relatively short section of 1000 km, which would be covered by a satellite in less than 2.5 min, with profiles separated by 50 km in 2000 m deep water would take three days to complete by a surface vessel. In a period of this length changes in the sea-surface topography, associated with ocean current variability, could introduce uncertainty in the comparison.

Alternatively an aeroplane dropping AXBTs (airborne expendable bathy-thermographs) could cover the same distance in less than three hours. However, the AXBTs measure only the temperature profile through the water column, and then only to a restricted maximum depth, typically 300 m. Consequently, for AXBTs to be used for the validation of altimeter measurements of surface topography, an accurate relationship between the measured truncated temperature profile and the total dynamic height must be known.

1.3. PREVIOUS RESULTS

Two published works compare the changes in the sea-surface topography of the Kuroshio Extension Current off Japan as measured by the SEASAT altimeter with those derived from repeated AXBT sections (Bernstein, Born and Whritner, 1982) and with repeated shipborne hydrographic surveys (Byrne and Pullen, 1983). Bernstein et al. used archived data to derive a relationship between the AXBT measurements and the sea-surface topography, while Byrne and Pullen used ship-launched, deep (to 1800 m) XBTs (expendable bathy-thermographs) with occasional CTD stations to provide the information relating temperature to specific volume. Both groups reported agreement at the level of $\sim$ 10 cm between hydrographic and altimetric topography changes. The measured topography itself changed by 40 to 60 cm in one to two weeks.

1.4. SCOPE OF THIS WORK

The purpose of this work is to explore the feasibility of using AXBT profiles between Scotland and Iceland as a method of validating the satellite altimeter sea-surface topography in this area. Historical oceanographic data are used to determine a relationship between truncated temperature profiles, as measured by AXBTs, and the surface topography—and this expression is tested using an independent CTD

data set. Additionally, historic atmospheric profiles are analysed to quantify the effects of atmospheric variability on the altimeter range measurement.

The motivation for these activities is the planned COMPASS experiment which will apply the new technique of using ground-based microwave transponders to obtain measurements of the position of the orbit of the GEOSAT satellite on a particular repeating arc from the Mediterranean Sea to Scotland. When used with an accurate orbit model these measurements could provide a determination of the GEOSAT arc with sufficient accuracy to permit, in principle, the monitoring of variations in the sea-surface topography between Scotland and Iceland. Ocean-current variability in this stretch of water is of direct relevance to the GIN Sea Programme of SACLANTCEN as well as to other oceanographic and climatological activities, such as the World Ocean Circulation Experiment (WOCE) of the World Climate Research Programme (WCRP) (e.g. Woods, 1985).

2. GEOSAT

GEOSAT is a US Navy satellite carrying a radar altimeter with characteristics and performance similar to the altimeter on SEASAT, a technical description of which is given by Townsend (1980).

In late 1986 GEOSAT was placed in an orbit in which the sub-satellite track repeats itself, to a cross-track accuracy of about 1 km at the earth's surface, every 17 days. The satellite orbit is about 800 km above the sea-surface and the orbit inclination is such that the world ocean is sampled between latitudes 72°N and 72°S. The precisely repeating orbit means that differences in the range signal can reveal changes in ocean currents in areas where the geoid is not known to sufficient accuracy for the absolute ocean topography to be determined.

GEOSAT is a single instrument satellite and consequently information required to make corrections to the range signal, as outlined in section 1.1, must be obtained from auxiliary sources of data. (Some other altimetric satellites, such as SEASAT and the European ERS-1 scheduled for launch in 1989, carry other instruments and the additional related data—such as the precipitable water vapour content from a microwave radiometer—can be used to correct, in part, the altimeter range signal.)

3. COMPASS

The COMPASS Project is a joint European–US experiment designed to use active, shore-based microwave transponders on the sub-satellite track of GEOSAT for the purpose of calibrating the altimeter range measurement (Rutherford Appleton Laboratory, 1987). Ground-based retroreflectors have been shown capable of providing reference data for an airborne altimeter (Powell, 1986), but COMPASS will provide the first opportunity of using transponders with a satellite altimeter. The accuracy of the altimeter range measurement over the transponders is confidently expected to have an rms error < 5 cm.

The project is being led by the Rutherford Appleton Laboratory in the UK (under contract to ESA, the European Space Agency), and NORDA in the US. The other European collaborating groups are at the Mullard Space Science Laboratory of University College London, the University of Leicester, the Institute of Oceanographic Sciences, the Admiralty Research Establishment in the UK, and the University of Delft in the Netherlands. Many of these groups share an interest in the subsequent use of transponders for calibrating the ERS-1 altimeter.

The first phase of COMPASS is planned to start in autumn of 1987 and is primarily a hardware test using transponders sited around the UK coastline under several GEOSAT arcs. At the start of 1988 the second phase, of at least six-months duration, will start—and it is planned that two transponders, sited near Rome and Aberdeen, will be used under a particular GEOSAT arc that runs from the Mediterranean Sea to Iceland and on over Greenland (Fig. 2). This arc passes over two enclosed shallow-water lakes, Grevelingen and Krammer, the levels of which are routinely and carefully monitored, and altimeter range measurements over their surfaces will provide a third independent measurement between the two transponders. Grevelingen Lake is about 1200 km from Rome and about 700 km from Aberdeen.

Results from analyses of data from repeating orbits of the SEASAT mission indicate that over length scales of about 2000 km the arcs are stable, and that after the application of a linear correction to each arc (the so-called bias and tilt correction), the measurements from collinear arcs can be superimposed in areas with small oceanographic signal to give a residual rms deviation of < 5 cm (rms) (Cheney et al., 1983). If the same is true for GEOSAT, and this can be tested using the measurements over Grevelingen and Krammer, then data from the repeating COMPASS arc will also reveal oceanic current variability in the Mediterranean section and between Scotland and Iceland, and possibly also in the Denmark Strait between Iceland and Greenland.

A number of collaborating groups intend to deploy oceanographic instrumentation at or near the GEOSAT sub-satellite track to provide independent in-situ measurements which will be used to validate the altimeter signal between Scotland and Iceland. This instrumentation will include tide gauges, current meter moorings and CTD/XBT sections, and will be concentrated on the Hebridean Shelf to Faeroes Bank region.

The prospect of making repeated sections of sea-surface topography across the major channels connecting the Greenland, Iceland and Norwegian Seas with the North Atlantic Ocean is very attractive to many oceanographic groups. In particular the data could be useful to the GIN Sea Programme of SACLANTCEN, by providing measurements through the 1987–88 winter and spring seasons, and complementing ship-borne and mooring data to be gathered during early summer of 1988.

The contribution of the SACLANTCEN Applied Oceanography Group (Project 23) to COMPASS is to establish the feasibility of using AXBT profiles to validate the altimeter data and, where possible, assist in the coordination of such AXBT flights and in the subsequent data analysis. This document reports on the initial feasibility study and also quantifies the errors caused by atmospheric variability along the COMPASS arc from Scotland to Iceland.

4. Thermohaline variability

The Equation of State of seawater defines density as a non-linear function of temperature, salinity and pressure (UNESCO, 1981; Pond and Pickard, 1983). The conventional method of obtaining a profile of density is to calculate it from measurements of temperature, electrical conductivity and pressure, from which salinity is derived as an intermediate result. The purpose of this section is to find an expression for the specific volume of seawater (the reciprocal of the density) as a function of temperature alone, for the limited range of conditions found between Scotland and Iceland. This expression, derived from historical data, will be tested against a set of independent CTD profiles from the SACLANTCEN GIN Sea cruise of June 1986.

The dynamic height anomaly between the surface and a pressure level P in a column of seawater is obtained by integrating the specific volume anomaly $\delta(S,T,P)$:

$$H_P = \int_0^P \delta(S,T,P)\,\mathrm{d}P = \int_0^P [\alpha(S,T,P) - \alpha(35,0,P)]\,\mathrm{d}P, \tag{1}$$

where α is the specific volume. Since for AXBT measurements only a temperature profile is available, and this does not generally penetrate the entire water column, we seek an estimator $\delta^*(T)$, such that H_P is well approximated by

$$H_P^* = \sum \delta^*(T_i) \cdot \Delta P_i. \tag{2}$$

4.1. HISTORICAL DATA

The historical data used in this study are from the global ocean climatology of Levitus (1982), which is a compilation of oceanographic station and profile data from the files of the National Oceanographic Data Center (NODC) in Washington DC. The data have been subjected to stringent quality control. The full resolution of the Levitus data is 1° in latitude and longitude, but those examined here are at the reduced resolution of 5°. These data were chosen because they are presented as statistics (i.e. mean values and variances) at standard pressure levels. Indeed Levitus presents tables of not only annual statistics (including variance) of temperature, salinity and specific volume anomaly (as well as other oceanographic variables) at the standard pressure levels throughout the water column, but also seasonal values at levels to 250 dbar. The pressure levels used by Levitus are at 10 m intervals from the surface to 50 m, then 75 m, 100 m, 125 m, 150 m, 200 m, 250 m, 300 m, and at 100 m intervals thereafter.

Alternative descriptions of mean temperature and salinity profiles in the world ocean have been presented by Emery and Dewar (1982), but their description is confined to the area south of 60°N in the North Atlantic Ocean. Consequently their data does not extend over much of the GEOSAT COMPASS arc. Furthermore, their approach was to describe the thermohaline variability of the oceans as a relatively small number of classes, which would inevitably lead to a loss of accuracy for the purposes of regional analyses such as this. However, they do demonstrate that for the N.E. Atlantic between 45° and 60°N, 20° to 50°E, it is possible to calculate 0 to 500 dbar dynamic heights in the mean, to an accuracy of about 2 dynamic cm* from temperature profiles alone. There is a slight loss of accuracy in using mean salinity profiles as functions of depth rather than as functions of temperature.

An initial examination of the Levitus data for the 5° box to the S.E. of Iceland centred at 62.5°N, 12.5°W, through which the northern part of the COMPASS arc passes, revealed an unphysical temperature–salinity (T-S) relationship in that the water column was significantly statically unstable in the mean. This is presumably caused by sampling biases in the distribution of the profiles for this box which would include measurements taken in water to the north of the Iceland-Faeroes Front as well as in the N. Atlantic water to the south. For example, at depth of 100 dbar, 2707 measurements of temperature pass Levitus's quality control tests to contribute to the mean value—but only 1679 values of salinity and 1528 values for measured specific volume anomaly pass the tests. The large T-S variability across the Front (standard deviation in temperature at 100 dbar is 7.56 K) and the non-linearity of the Equation of State, exacerbated by the absence of a strict correspondence between measured variables, could well explain the observed mean instability.

The COMPASS arc also passes through the box centred at 62.5°N, 7.5°W, and while the mean specific volume anomaly profile in this box is statically stable, the values are more characteristic of those in areas to the northeast in the Norwegian Sea than to those in the Atlantic Ocean. Since the COMPASS arc passes over the Atlantic water it was decided instead to use data from the box centred at 62.5°N, 17.5°W as being more characteristic of the required thermohaline properties. Even here, however, the observed annual mean specific volume anomaly does not decrease monotonically with depth, but the resulting instability is marginal.

The annual mean profiles of temperature (T) and salinity (S) from the surface to 500 dbar are shown in Fig. 3, with the envelope of ± 1 standard deviation at each pressure level. These profiles have been generated by joining the values at the standard pressure levels given by Levitus with straight lines. Much of the thermohaline variability is concentrated in the top 100 dbar, both in the annual data and in the seasonal profiles (Fig. 4). In particular the salinity variability is

* The dynamic metre has units of 10 $m^2 s^{-2}$ and is a unit of geopotential, i.e. energy divided by mass. Numerically it approximates very well to the linear metre.

much reduced below 80–100 dbar. The seasonal change in the mean salinity below 100 dbar is < 0.1 ppt. The annual mean T-S relationship from the surface to 1500 dbar is shown in Fig. 5, with the marginal static stability apparent at the salinity maximum (at a pressure of about 125 dbar).

An estimate of the proportion of the total specific volume anomaly variability that can be described with temperature profiles alone can be derived by calculating the specific volume anomaly for mean values of temperature and salinity adjusted in turn by ±1 standard deviation. Figure 6 is a profile of the quantity

$$\frac{(\delta(\overline{T}+T',\overline{S},P)-\delta(\overline{T}-T',\overline{S},P))}{(\delta(\overline{T},\overline{S}+S',P)-\delta(\overline{T},\overline{S}-S',P))} \simeq \left(\frac{\partial\delta}{\partial T}\right) \mathrm{d}T \Big/ \left(\frac{\partial\delta}{\partial S}\right) \mathrm{d}S,$$

where overbars denote mean values, and primes denote standard deviations. Between 10 and 400 dbar, where most of the variability occurs, accurate measurements of temperature variability could describe between 60% and 80% of the expected specific volume anomaly variability. The effects on calculated dynamic heights of the observed temperature and salinity variabilities are given in Table 2.

TABLE 2

The effects on dynamic height of measured temperature and salinity variability (using annual data for the 5° square centred at 62.5°N, 17.5°W; Levitus, 1982)

Pressure range (dbar)	Changes in dynamic height[a] (dynamic cm)		
	$\Delta\delta(T')$	$\Delta\delta(S')$	$\lvert\Delta\delta(T')/\Delta\delta(S')\rvert$
0–300	4.78	−2.26	2.12
0–600	7.03	−3.52	2.00
0–1500	13.96	−7.30	1.91

[a] $\Delta\delta(T')$ is the change in dynamic height caused by an increase in temperature of one standard deviation at each level.
$\Delta\delta(S')$ is the change in dynamic height caused by an increase in salinity of one standard deviation at each level.

The form of the dependence of the mean specific volume anomaly on the mean temperature is shown in Fig. 7, for the annual case from the surface to 1500 dbar, and for seasonal values from the surface to 250 dbar. The curves shown here are for specific volume anomalies calculated from the mean temperatures and salinities at each pressure, but they are substantially similar to those of mean measured specific volume anomaly given by Levitus. The annual mean profile, $\overline{\delta}(\overline{T})$ has three

parts: (a) from the surface to $P \sim 100$ dbar $\bar{\delta}$ shows a quadratic dependence on temperature; (b) from $P \sim 100$ dbar to $P \sim 600$ dbar $\bar{\delta}$ is practically constant; and (c) for $P > 600$ dbar $\bar{\delta}$ is approximately a linear function of temperature. The seasonal mean profiles all converge on the constant $\bar{\delta}$-value below $P \sim 100$ dbar. The mean profiles for spring and summer also follow a similar quadratic temperature dependence in the upper ocean. For the summer case the temperature dependence is significantly different from the annual mean, and this indicates the need for seasonally distinct expressions for relating specific volume anomaly to temperature. However, the mean profiles for autumn and for winter are significantly statically unstable. This is most likely caused by sampling biases in the temperature and salinity data and these profiles cannot be taken to represent realistically the condition of the ocean.

The annual, spring and summer mean profiles of $\bar{\delta}$ show a large change between $P = 0$ and 10 dbar. This can be traced back to the markedly fresher layer of surface water in the mean salinity profiles. Although this fresh surface layer is physically reasonable, in the sense that it does not destabilize the water column, it is rather unlikely to be real—given the absence of large river run-off or ice-melt in that area. The consequence for the form of the temperature dependence of the specific volume anomaly is to cause large changes at higher temperatures, which can give rise to unphysical values of $\bar{\delta}$ at measured temperatures above those on the curves of Fig. 7. Thus when fitting a quadratic curve to the upper part of the $\bar{\delta}(\overline{T})$ curve the values at $P = 0$ were discarded.

Expressions relating mean specific volume anomalies to measured temperature are given in Table 3, for both the measured specific volume anomaly and that calculated from the mean temperature and salinity profile. The expressions for spring and summer merge into the annual profile at or above pressures of 250 dbar. Since the autumn and winter data lead to unstable profiles, the annual expression should be used for these seasons.

4.2. COMPARISON WITH GIN86 DATA

The positions of CTD stations taken during the GIN Sea 86 cruise of the HNLMS Tydeman are shown in Fig. 8, and those to the south of the Faeroe Islands were chosen as independent test data for the $\delta^*(T)$ expressions of Table 3. Twenty-seven stations lying in the area defined by latitude south of 62°N, longitude west of 6°W were selected (stations CTD12 to CTD38) and dynamic height profiles were calculated using the UNESCO (1981) formulae (Hopkins et al., 1987). The dynamic height contours for the layers 0 to 300 dbar and 0 to 600 dbar are shown in Fig. 9. Because of water depth limitations, there are only 20 stations extending to $P > 250$ dbar and 14 to $P > 600$ dbar.

The sea-surface topography to the southwest of the Faeroes, as portrayed by the 0–

TABLE 3
Models for specific volume anomaly

(a) Measured $\delta(S,T,P)$

Annual mean	$\delta^* =$	$\begin{cases} 10.195 - 2.148T + 0.153T^2, & \text{for } T > 8.40^\circ\text{C} \\ 0.680, & \text{for } 8.40^\circ\text{C} \geq T \geq 7.63^\circ\text{C} \\ 0.199 + 0.063T, & \text{for } 7.63^\circ\text{C} > T \end{cases}$
Spring mean	$\delta^* =$	$\begin{cases} 3.114 - 0.770T + 0.057T^2, & \text{for } T > 8.46^\circ\text{C} \\ 0.680, & \text{for } 8.46^\circ\text{C} \geq T \geq 7.63^\circ\text{C} \\ 0.199 + 0.063T, & \text{for } 7.63^\circ\text{C} > T \end{cases}$
Summer mean	$\delta^* =$	$\begin{cases} 5.167 - 1.111T + 0.069T^2, & \text{for } T > 9.12^\circ\text{C} \\ 0.199 + 0.063T, & \text{for } 9.12^\circ\text{C} \geq T \end{cases}$
Autumn/Winter mean (as annual)	$\delta^* =$	$\begin{cases} 10.195 - 2.148T + 0.153T^2, & \text{for } T > 8.40^\circ\text{C} \\ 0.680, & \text{for } 8.40^\circ\text{C} \geq T \geq 7.63^\circ\text{C} \\ 0.199 + 0.063T, & \text{for } 7.63^\circ\text{C} > T \end{cases}$

(b) Calculated $\delta(S,T,P)$

Annual mean	$\delta^* =$	$\begin{cases} 9.273 - 2.172T + 0.137T^2, & \text{for } T > 8.45^\circ\text{C} \\ 0.680, & \text{for } 8.45^\circ\text{C} \geq T \geq 7.81^\circ\text{C} \\ 0.180 + 0.064T, & \text{for } 7.81^\circ\text{C} > T \end{cases}$
Spring mean	$\delta^* =$	$\begin{cases} 6.105 - 1.428T + 0.093T^2, & \text{for } T > 8.46^\circ\text{C} \\ 0.680, & \text{for } 8.46^\circ\text{C} \geq T \geq 7.81^\circ\text{C} \\ 0.180 + 0.064T, & \text{for } 7.81^\circ\text{C} > T \end{cases}$
Summer mean	$\delta^* =$	$\begin{cases} 3.373 - 0.740T + 0.050T^2, & \text{for } T > 8.34^\circ\text{C} \\ 0.680, & \text{for } 8.34^\circ\text{C} \geq T \geq 7.81^\circ\text{C} \\ 0.180 + 0.064T, & \text{for } 7.81^\circ\text{C} > T \end{cases}$
Autumn/Winter mean (as annual)	$\delta^* =$	$\begin{cases} 9.273 - 2.172T + 0.137T^2, & \text{for } T > 8.45^\circ\text{C} \\ 0.680, & \text{for } 8.45^\circ\text{C} \geq T \geq 7.81^\circ\text{C} \\ 0.180 + 0.064T, & \text{for } 7.81^\circ\text{C} > T \end{cases}$

600 dbar dynamic heights (H_{600}) shows a peak-to-peak signal of over 10 dynamic cm (the standard deviation of the 14 stations is 4.2 dynamic cm), while that detected by CTD measurements extending only to 300 dbar (H_{300}) is much reduced (standard deviation of 20 stations is 1.1 dynamic cm). However, the two sets of data are well correlated ($R^2 = 0.95$) as can be seen by the similarity in the contours of Fig. 9, and H_{600} can be predicted from H_{300} by

$$H_{600} = 3.76H_{300} - 40.20. \tag{3}$$

This expression, derived by linear regression, has a standard error of 0.95 dynamic cm.

The H^{*}_{300} field was predicted from the measured temperature profiles to 300 dbar, using the expressions given in Table 3. The data were taken between 11 to 13 June 1986, and so the spring season expressions (derived from measurements in May, June and July) were used. For comparison H^{*}_{300} was also computed using the annual expressions. The results of the comparison between the predicted and measured 0–300 dbar dynamic heights are summarized in Table 4. The errors are those resulting solely from the prediction and are additional to those caused by measurement inaccuracies in the temperature profile from the AXBT or XBT.

TABLE 4

Errors in 0–300 dbar dynamic heights predicted from temperature profiles

(a) Measured $\delta(S,T,P)$

Algorithm[a]	Errors (dynamic cm)	
	Mean	Standard deviation
annual	1.26	1.98
spring	0.56	1.22

(b) Calculated $\delta(S,T,P)$

Algorithm[a]	Errors (dynamic cm)	
	Mean	Standard deviation
annual	1.15	1.81
spring	0.79	1.33

[a] See Table 3.

4.3. DISCUSSION

From Table 4 it can be seen that in the case studied here a seasonally adjusted algorithm gives a more accurate prediction of the 0–300 dbar dynamic heights from temperature data alone than an annual expression does. For both the spring and annual algorithms, those derived using values of $\delta(\overline{S},\overline{T}\ P)$, i.e. calculated from mean profiles of salinity and temperature, are better predictors than those derived from $\overline{\delta}(S,T,P)$, i.e. the mean profile of measured specific volume anomaly.

However even in the best case the errors are comparable to the expected signal in H_{300}. The spatial distribution of the errors (Fig. 10) is coherent, and could be easily misinterpreted as signal. In this case, the large errors to the south are associated with an increase in near-surface salinity of 0.01 ppt. As a consequence the use of AXBT/XBT profiles alone to validate satellite measurements of sea-surface topography cannot be expected to be without problems, and will require additional information on the spatial variability of the T-S relationship, such as that from CTD profiles.

5. Atmospheric variability

By influencing the refractive index of the atmosphere along the path of the radar altimeter pulse, variations in the atmospheric structure significantly modify the radar range measurement. A correction can be applied if the structure of the atmosphere is known along the radar path. This will be necessary for the COMPASS transponder measurements. Variations in the atmosphere, both spatial and temporal, could lead to errors in the satellite measurements of the sea-surface topography.

The purpose of this section is to quantify these errors by examining historical atmospheric measurements from the COMPASS area.

5.1. RANGE ERRORS CAUSED BY THE ATMOSPHERE

The effects of the atmosphere on the radar altimeter absolute range measurement can be conveniently considered in three parts: the dry atmospheric effect, the wet tropospheric effect, and atmospheric loading (inverse barometer effect). The dry atmospheric effect can be expressed as a function of the surface pressure (and therefore contains a contribution from the water vapour molecules), but to calculate the wet tropospheric effect, which is dependent on the temperature of the water vapour, requires knowledge of the atmospheric temperature and humidity profiles.

The dry atmospheric range correction, in m, is given by

$$\Delta h_d = 2.276 \times 10^{-3} P_0, \tag{4}$$

where P_0 is the surface pressure in mbar (Smith and Weintraub, 1953). Hopfield (1971) has shown that this expression is accurate to 0.2% (i.e. $\sim$ 0.5 cm).

The wet tropospheric range correction is calculated from

$$\Delta h_w = 1.7227 \int \frac{\rho_w(z)}{T} \, dz, \tag{5}$$

or

$$\Delta h_w = 1.7227 \sum \frac{\rho_w(z)}{T} \Delta z, \tag{6}$$

where ρ_w is the atmospheric water density in kg m^{-3} (Stewart, 1985).

For both cases it has been assumed that the atmosphere behaves as an ideal gas and the local variation in the value of the acceleration due to gravity at the sea-surface has been neglected.

TABLE 5
Altimeter range errors due to atmospheric variability

Season	Number of radiosondes	Wet (cm)	Dry (cm)	Total (cm)
May–Jul	87	10.2 + 3.5	230.1 ± 1.3	1261.8 ± 7.8
Aug–Oct	75	9.7 ± 3.4	229.8 ± 1.3	1259.5 ± 7.8
Nov–Jan	85	5.5 ± 2.3	230.2 ± 1.7	1257.3 ± 9.5
Feb–Apr	80	5.2 ± 2.0	229.9 ± 1.5	1255.4 ± 8.8

Derived from quality-controlled radiosondes from the area 58°N to 65°N, 20°W to 0°E. The values are mean ±1 standard deviation. The total also includes the atmospheric loading effect.

The atmospheric loading, or inverse barometer effect, is given in m by

$$\Delta h_P \approx 0.0101 P_0 \tag{7}$$

when P_0 is in mbar. This effect is simply the response of the mean sea-level to changes in the atmospheric pressure. It is thus not an error in the sense that it corrupts the altimeter range measurement, but it does introduce an error if the sea-surface topography is interpreted solely in terms of geostrophic currents. There is a time constant associated with the dynamic ocean response to a changing surface pressure field, but for the purposes of this work the response is assumed to be instantaneous.

5.2. ATMOSPHERIC PROFILES

The atmospheric conditions used in this study were extracted from a large set of profiles through the marine atmosphere derived from radiosonde ascents from ships and coastal and island weather stations. The original data set consists of profiles from the northeast Atlantic Ocean and the GIN Sea area, which have been subjected to stringent quality control (Minnett, Eyre and Pescod, 1986 and 1987). Those used here were restricted in their geographical range to latitudes between 58° and 65°N and longitudes between 20°W and 0°E, and were grouped into seasons corresponding to the same months as the Levitus oceanographic data.

5.3. ALTIMETER RANGE ERRORS

The altimeter range error components were calculated for each profile, as discussed above, and the seasonal statistics are given in Table 5, with histograms of the Δh_w and total range error in Fig. 11.

The dry range error Δh_d can be corrected to an accuracy of better than 0.02 m by adding 2.30 m to the altimeter measurements, while the wet range error Δh_w can be corrected to better than 0.04 m by adding a seasonally varying value.

The main component of the variability of the total atmospheric effect is, however, the atmospheric loading—and to correct this will require the surface air pressure. If the air pressure is accurately known the atmospheric loading can be corrected to the (unknown) limit imposed by the dynamic response of the ocean.

5.4. DISCUSSION

To reduce all atmospheric range errors to below the ±2 cm accuracy expected of the COMPASS transducer measurement, it will be necessary to know the surface air pressure and atmospheric structure—not only at the transducer locations at the time of the satellite overpass but also along the sub-satellite track.

Surface pressure measurements at the transponder site can be made accurately using a standard barometer, but measurements of the atmospheric stucture will require radiosonde ascents synchronized with the satellite measurement. An analysis of atmospheric profiles taken from ships during the JASIN (Joint Air Sea Interaction) Experiment in the autumn of 1978 at about 60°N, 12.5°W (Pollard, Guymer and Taylor, 1983) revealed a loss of correlation in the precipitable water after intervals of 24 h, with a decay of the autocorrelation function to values of 0.9 after about 3 h (Fig. 12).

The precipitable water w is closely linked to the wet tropospheric range error:

$$\Delta h_w \propto \frac{w}{T_a}, \tag{8}$$

where T_a is a representative air temperature in the troposphere (Stewart, 1985). Thus the correlation periods of precipitable water can be expected to be similar to those of Δh_w. As a consequence radiosonde measurements intended to determine Δh_w at the COMPASS transponder location should be taken within 3 h of the satellite overpass.

The spatial variability of precipitable water may, if not known to adequate accuracy, be mapped into sea-surface topography variations. An example of the precipitable water distribution in this area is shown in Fig. 13, which is derived from measurements of the SEASAT Scanning Multichannel Microwave Radiometer (SMMR), also for the period of the JASIN Experiment (Taylor et al., 1983). Values of precipitable water near the position of the COMPASS arc vary from $> 30\ \mathrm{kg\,m^{-2}}$ to $< 12\ \mathrm{kg\,m^{-2}}$. For comparison the standard deviations of precipitable water calculated from the radiosondes used to derive Δh_w given in Table 5 range from $3.21\ \mathrm{kg\,m^{-2}}$ in winter to $5.68\ \mathrm{kg\,m^{-2}}$ in spring. This would appear to indicate that

the variability in Δh_w characteristic of the radiosonde locations could be encountered along a given single GEOSAT COMPASS arc, and unless corrected could produce range errors comparable to the sea-surface topography signal.

The problem of describing the spatial variability of the wet tropospheric range correction along the sub-satellite point is not trivial. One approach could be to have a series of radiosonde launches along the track, but bearing in mind the requirement of close temporal correspondence, this would require several ships positioned between Scotland and Iceland. Furthermore, the accuracies of individual radiosonde profiles may not be adequate. For example, random errors at the 10% level, while not contributing significantly to the statistics given in Table 5 (provided there is no systematic measurement error in the radiosondes making up the data set) could produce significant residual errors for individual ascents.

Another approach would be use the analysis fields from synoptic meteorological measurements or forecast fields. However there are not many reporting stations in this area, and humidity profiles are difficult to forecast accurately. The characteristics of the residual wet tropospheric range error would then be dominated by the error characteristics of the analysis or forecast field.

An alternative approach is to resort to measurements from instruments on other spacecraft. The infrared radiometers on current operational satellites and the microwave radiometers on proposed satellites could both provide measurements of precipitable water (w) which could be used to determine the wet tropospheric range correction. The TIROS Operational Vertical Sounder (TOVS, in which TIROS stands for Television and Infrared Observation Satellite) is a suite of radiometers on the present generation of weather satellites operated by NOAA (the US National Oceanic and Atmospheric Administration) and designed to measure atmospheric profiles of temperature and humidity. Current estimates of the accuracy of the retrieval of w is $< 1\ \mathrm{kg\,m^{-2}}$ (Chedin, 1986), when compared with radiosonde ascents from European stations in March 1982 in conditions of up to 30% cloud cover. The mean value of w for the 66 cases considered was $8.5\ \mathrm{kg\,m^{-2}}$. Since there are two such polar-orbiting satellites in operation at any time there is the possibility at these latitudes of having about 12 potentially useful overpasses each day, one of which should be within a few hours of the GEOSAT overpass. The spatial resolution of the water vapour retrieval is about 40 km.

A more accurate determination of w will become possible with the launch of the Special Sensor Microwave/Imager (SSM/I) on the next DMSP satellite (US Defense Meteorological Satellite Program). Numerical simulations predict an all-weather retrieval accuracy of $< 1\ \mathrm{kg\,m^{-2}}$ at a resolution of about 70×45 km (Hollinger and Lo, 1983). Although the retrieval is predicted to be very accurate, there is the possibility of a significant time interval between SSM/I and GEOSAT overpasses as there will be only one SSM/I in orbit and only two (fortuitously three) samples of the COMPASS arc area per day. The first SSM/I was successfully launched in

June 1987 and began operation in July. The SSM/I data are currently subject to calibration and validation.

Spatial variations in the surface atmospheric pressure could also induce surface undulations, which—while being legitimate variations in the sea-surface topography—may lead to erroneous estimations of surface geostrophic currents (unless the surface patterns are stationary over many days). Accurate knowledge of the surface pressure field would permit a correction (assuming rapid dynamic response of the ocean), and the most readily available source of such information would be surface meteorological analysis or forecast charts. As in the case of using meteorological fields to give the wet tropospheric correction, the error statistics of the analysis or forecast fields in this area would also contribute to the residual inaccuracies in the corrected surface current field.

6. Conclusions

The feasibility of using AXBTs or XBTs to validate the measurement of sea-surface topography from the GEOSAT altimeter during the COMPASS Experiment has been explored, and the results have been presented together with a quantification of the range errors resulting from atmospheric variability. The main conclusions are:

(1) There is a measurable signal in the sea-surface topography under the COMPASS arc from Scotland to Iceland, but its amplitude, > 10 cm (as shown in the 0–600 dbar dynamic height field), is small compared with oceanographic signals in other areas, such as at Western Boundary Currents (Table 1).

(2) Atmospheric variability, both temporal and spatial, could mask the oceanographic signal unless corrections are applied very carefully. As the first step, the dry atmospheric effect can be corrected by a constant offset, the wet tropospheric effect by a seasonally varying offset, and the inverse barometer effect by use of a meteorological chart. To be certain of reducing atmospheric effects to well below the level of the expected signal it will be necessary to apply more appropriate corrections. If radiosonde ascents are to be used to determine the wet tropospheric effect, they must be made within three hours of the satellite overpass—but cannot be presumed to be applicable for the whole length of the arc.

(3) Validation of the satellite altimeter measurement of sea-surface topography by AXBTs or XBTs alone is questionable. Although a good linear relationship exists between the dynamic heights of the 0–600 dbar and 0–300 mbar layers, to an accuracy of < 1 dynamic cm or < 25% of the signal, the 0–300 dbar dynamic height cannot be determined to sufficient accuracy from temperature data alone. Although most of the dynamic height variation is caused by temperature variability. Additional information, such as from CTD profiles, is required in order to specify the spatial variations in the relationship between temperature and salinity.

(4) A seasonally-dependent algorithm relating specific volume anomaly to temperature in this area is more accurate than an annually applicable one. The form of the dependency of specific volume on temperature is quadratic in the surface layers, constant at mid-depth, and linear in the deeper layers (Table 3).

References

BERNSTEIN, R.L., BORN, G.H. and WHRITNER, R.H. SEASAT altimeter determination of ocean current variability. *Journal of Geophysical Research*, **87**, 1982: 3261–3268.

BORN, G.H., WUNSCH, C. and YAMARONE, C.A. TOPEX: Observing the oceans from space. *EOS*, **65**, 1984: 433–434.

BYRNE, H.M. and PULLEN, P.E. Seasat-derived ocean surface topography: comparison with coincident Kuroshio hydrographic data. *Journal of Geophysical Research*, **88**, 1983: 2621–2625.

CHEDIN, A. Retrievals of atmospheric water vapour and surface temperature: preliminary results. Section 4.5.2.2 of 'Co-operative Studies of Climate Transients' by P.J. Minnett and H. Grassl. Report STI-022-J-C to Commission of the European Communities, Brussels. In press (1986).

CHENEY, R.E., MARSH, J.G. and BECKLEY, B.D. Global mesoscale variability from collinear tracks of SEASAT altimeter data. *Journal of Geophysical Research*, **88**, 1983: 4343–4354.

EMERY, W.J. and DEWAR, J.S. Mean temperature-salinity, salinity-depth and temperature-depth curves for the North Atlantic and North Pacific. *Progress in Oceanography*, **11**, 1982: 219–305.

HOLLINGER, J.P. and LO, R.C. SSM/I project summary report, NRL Memorandum 5055. Washington, DC, Naval Research Laboratory, 1983.

HOPFIELD, H.S. Tropospheric effect on electromagnetically measured range: prediction from surface weather data. *Radio Science*, **6**, 1971: 357–367.

HOPKINS, T.S. et al, 1987 The Atlantic Inflow Experiment – GIN Sea '86 Cruise of *HNLMS Tydeman*. Part 1: CTD/Rosette data report. SACLANTCEN Report, (in preparation).

LEVITUS, S. Climatological atlas of the world ocean, NOAA Professional Paper 13. US Department of Commerce, National Oceanic and Atmospheric Administration, 1982.

MINNETT, P.J., EYRE, J.R. and PESCOD, R.W. The marine atmosphere over the north eastern Atlantic Ocean, Chilton, Oxfordshire, UK, Rutherford Appleton Laboratory, RAL-86-044, 1986.

MINNETT, P.J., EYRE, J.R. and PESCOD, R.W. The variability of the North Atlantic marine atmosphere and its relevance to remote sensing. *International Journal of Remote Sensing*, **8**, 1987: 871–880.

POLLARD, R.T., GUYMER, T.H. and TAYLOR, P.K. Summary of the JASIN 1978 field experiment. *Philosophical Transactions of the Royal Society of London*, **A308**, 1983: 221–230.

POND, S. and PICKARD, G.L. Introductory Dynamical Oceanography, 2nd ed. Oxford, Pergamon, 1983.

POWELL, R.J. Relative vertical positioning using ground-level transponders with the ERS-1 altimeter. *IEEE Transactions on Geoscience and Remote Sensing*, **24**, 1986: 421–425.

RUTHERFORD APPLETON LABORATORY. COMPASS – a collaborative European-USA project to investigate the combined use of satellite altimeters and land-based transponders to study ocean tides and currents. *Chilton, Oxfordshire, UK, Rutherford Appleton Laboratory*, 1987.

SMITH, E.K. and WEINTRAUB, S. The constants in the equation for atmospheric refractive index at radio frequencies. *Proceedings of the I.R.E.*, **41**, 1953: 1035–1037.

STEWART, R.H. Methods of Satellite Oceanography. Berkeley, University of California Press, 1985.

TAYLOR, P.K. Atmospheric measurements for satellite altimetry. Presented at NATO Workshop on 'Satellite altimetry and ocean circulation', San Miniato, Italy, 11–14 April, 1983.

TAYLOR, P.K., GUYMER, T.H., KATSAROS, K.B. and LIPES, R.C. Atmospheric water distributions determined by the Seasat multi-channel microwave radiometer. *In:* Variations in the Global Water Budget. Street-Perrott, A., Beran, M. and Ratcliffe, R., eds. Dordrecht, Reidel, 1983: pp. 93–106.

TOWNSEND, W.F. An initial assessment of the performance achieved by the Seasat-1 radar altimeter. *IEEE Journal of Oceanic Engineering*, **5**, 1980: 80–92.

UNESCO. Tenth report of the Joint Panel on Oceanographic Tables and Standards. *UNESCO Technical papers in Marine Science*, no. 36.

WOODS, J.D. The world ocean circulation experiment. *Nature*, **314**, 1985: 501–511.

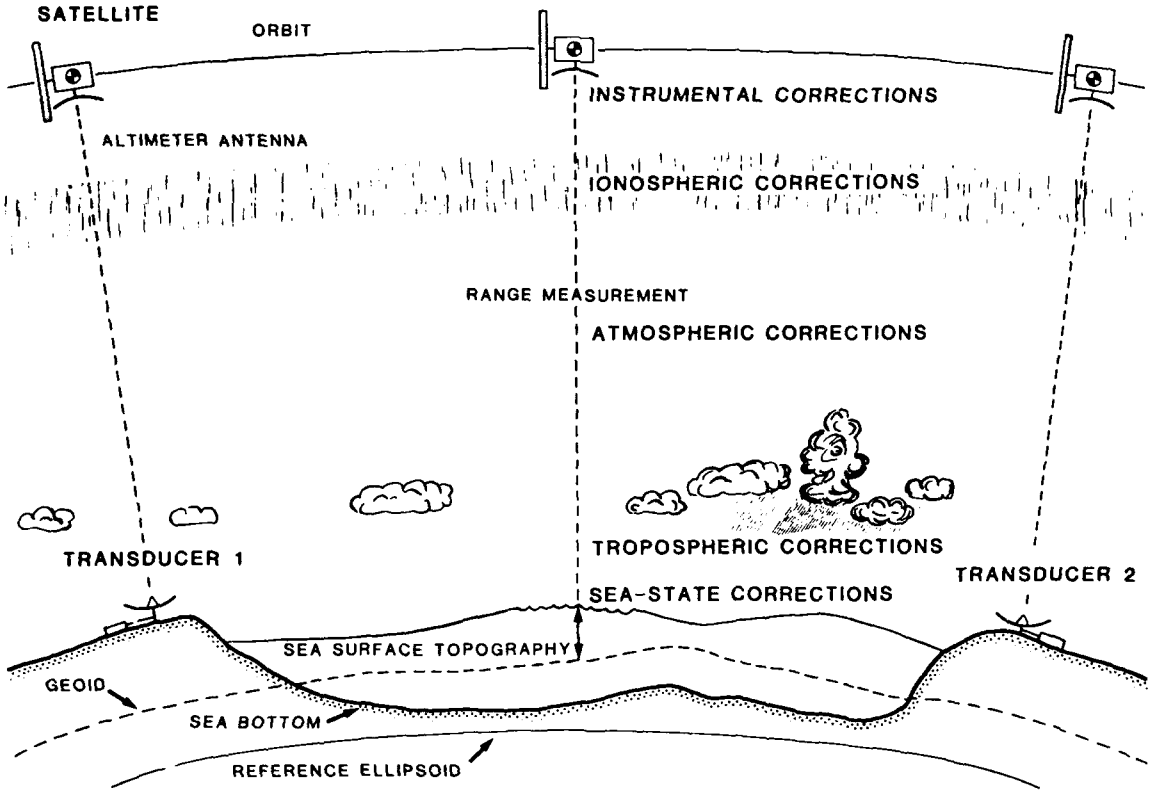

Fig. 1: Schematic representation of the satellite altimeter measurement of the sea-surface topography with the use of coastline transponders, and the necessary corrections required for accurate range measurements.

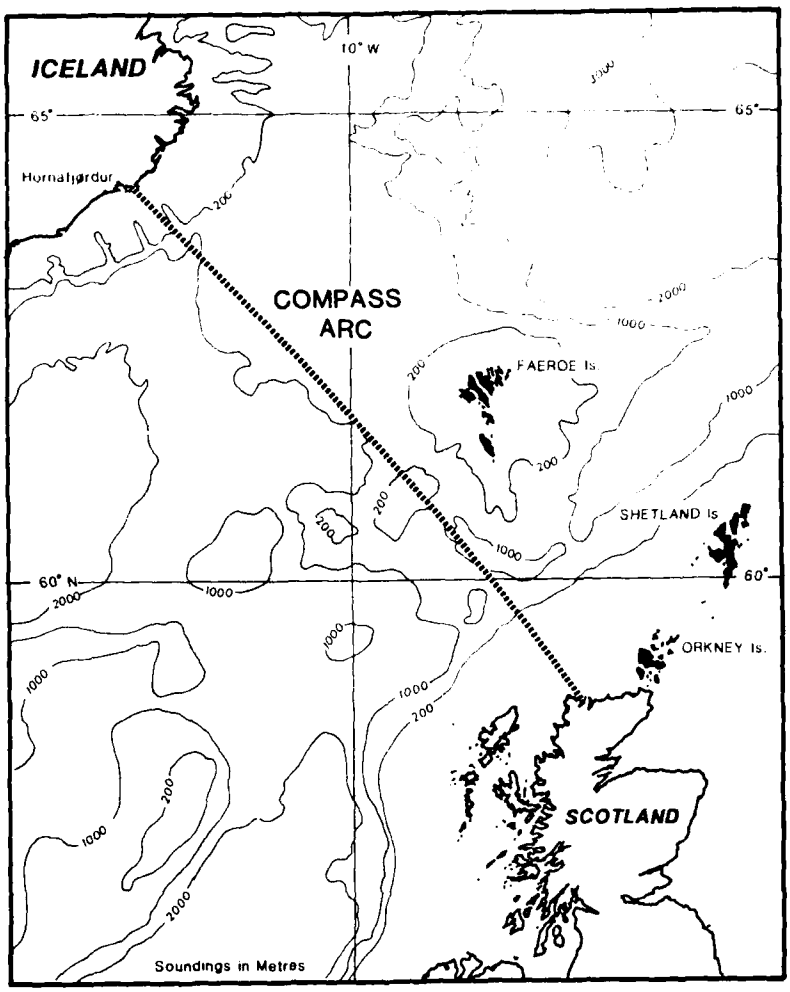

Fig. 2: Showing the position of the COMPASS arc of GEOSAT between Scotland and Iceland. The arc will be repeated to a nominal 1 km cross-track accuracy every 17 days. The full length of the arc extends from the N. African coast to Greenland, with the active transponders sited off Rome, Italy, and Aberdeen, Scotland.

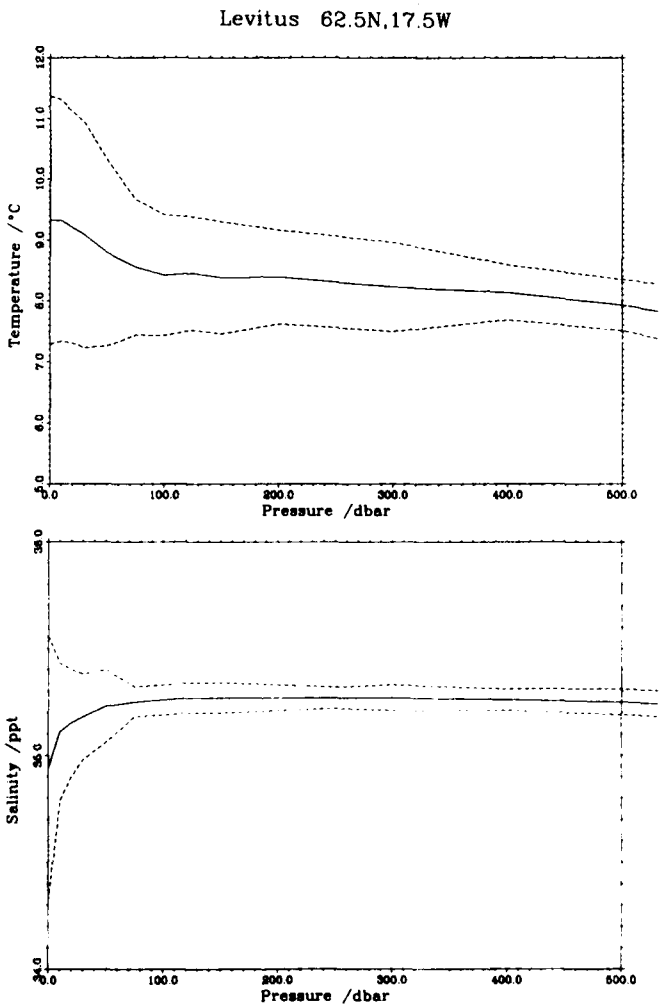

Fig. 3: Annual mean profiles of temperature and salinity from the surface to P = 500 mbar for the 5° × 5° latitude–longitude box centred at 62.5°N, 17.5°W. The dashed lines mark ±1 standard deviation. The data are taken from the Levitus (1982) compilation.

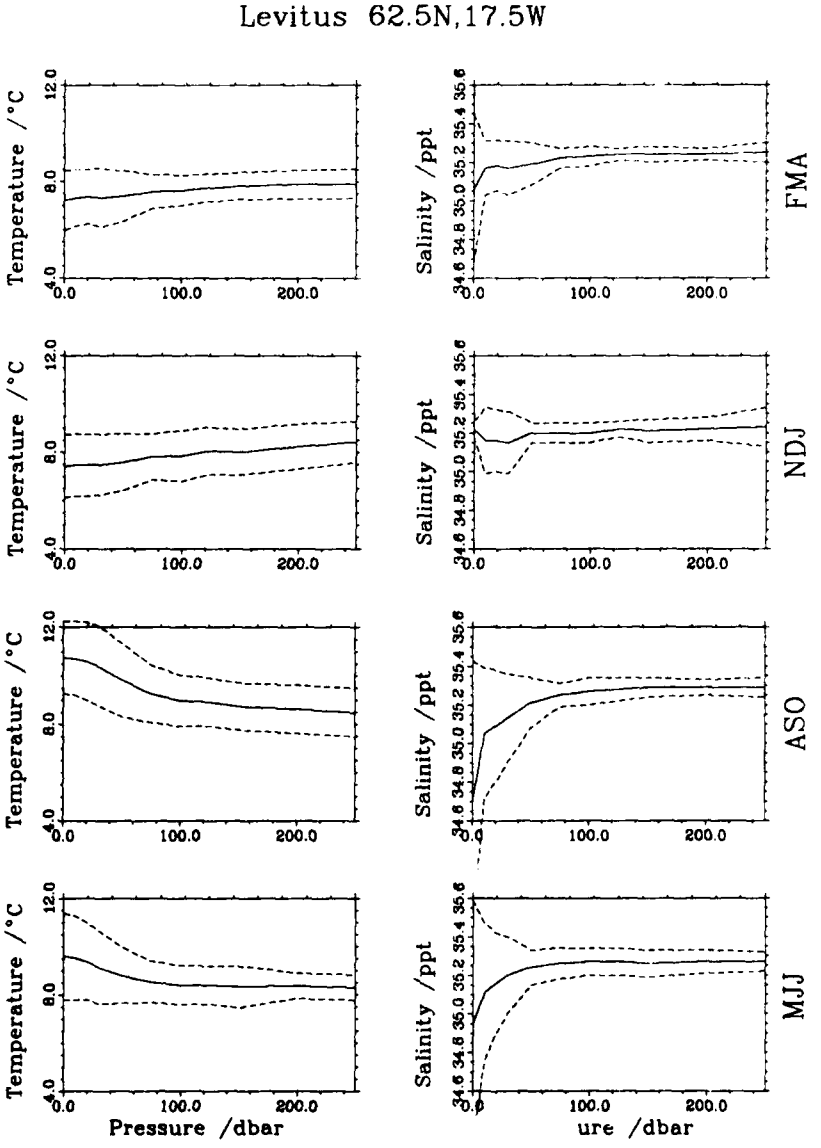

Fig. 4: As Fig. 3, but showing the seasonal me profiles of temperature and salinity from the surface to P = 250 mbar. (MJJ: May l; ASO: Aug-Oct; NDJ: Nov-Jan; FMA: Feb-Apr.)

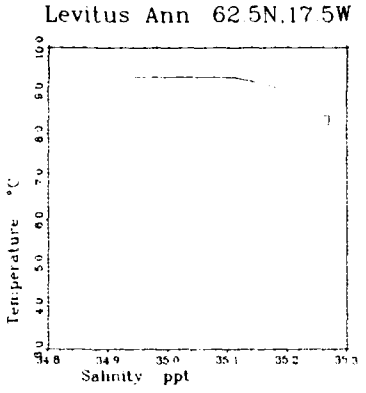

Fig. 5: As Fig. 3, but showing the annual mean temperature salinity relationship between the surface to $P = 1500$ dbar. The pressure of the salinity maximum is about 125 dbar, at which value a slight hydrostatic instability is apparent. The strong near-surface salinity gradient is caused by a suspect value at $P = 0$ dbar (see text).

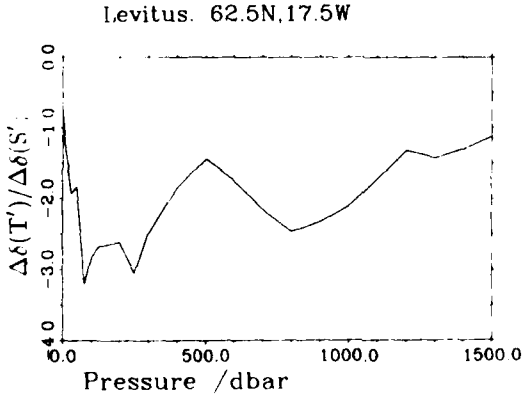

Fig. 6: The ratio of the variabilities (standard deviations) in calculated specific volume anomalies caused by the observed variabilities of temperature and salinity. The data are those used for Fig. 3.

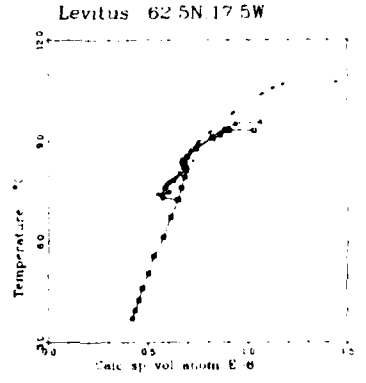

Fig. 7: The dependence of calculated specific volume anomaly on temperature. The data are those used for Figs. 3 and 4. The mean profile (□) extends from the surface to $P = 1500$ dbar. The seasonal profiles, from the surface to $P = 250$ dbar, are denoted as follows: spring (May-Jul), △; summer (Aug-Oct), +; autumn (Nov-Jan), ×; winter (Feb-Apr), ◇ The symbols show the positions of the standard depth levels used by Levitus: 0, 10, 20, 30, 40, 50, 75, 100, 125, 150, 200, 250, 300, 400, 500, 600, 700, 800, 900, 1000, 1100, 1200, 1300, 1400, and 1500 m.

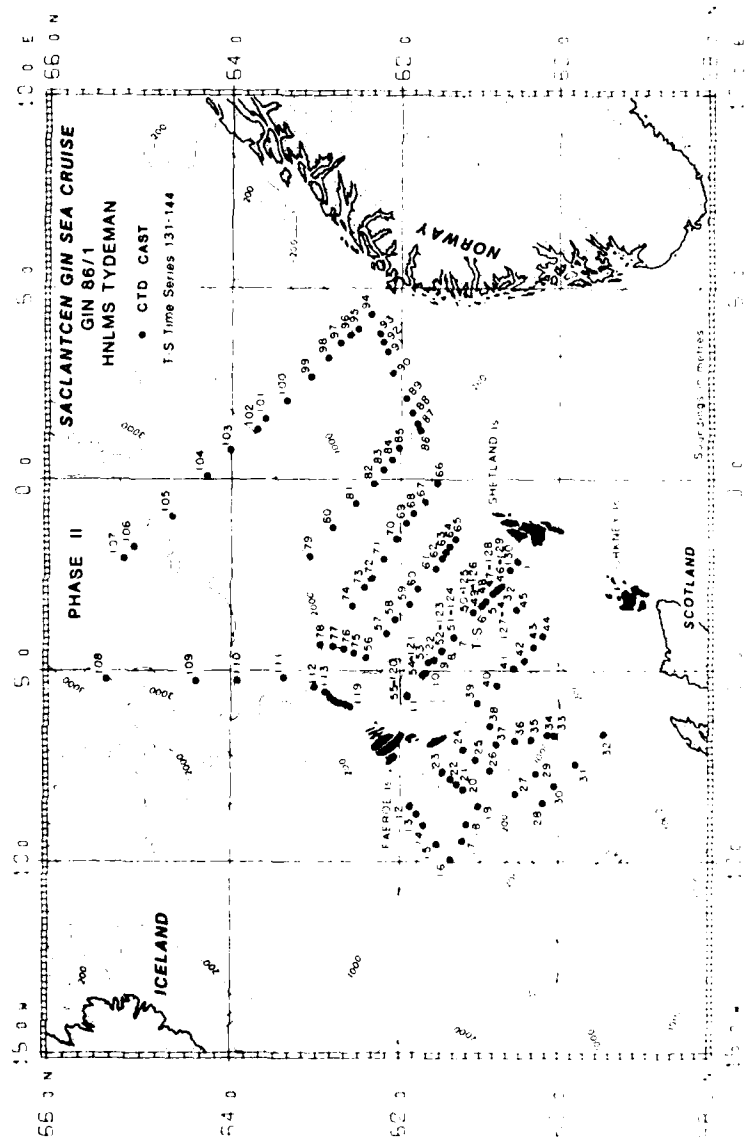

Fig. 8. Showing the positions of CTD stations of the GIN Sea '86 cruise of the *HNLMS Tydeman* from 9 to 25 June 1986. [From Hopkins et al., 1987.]

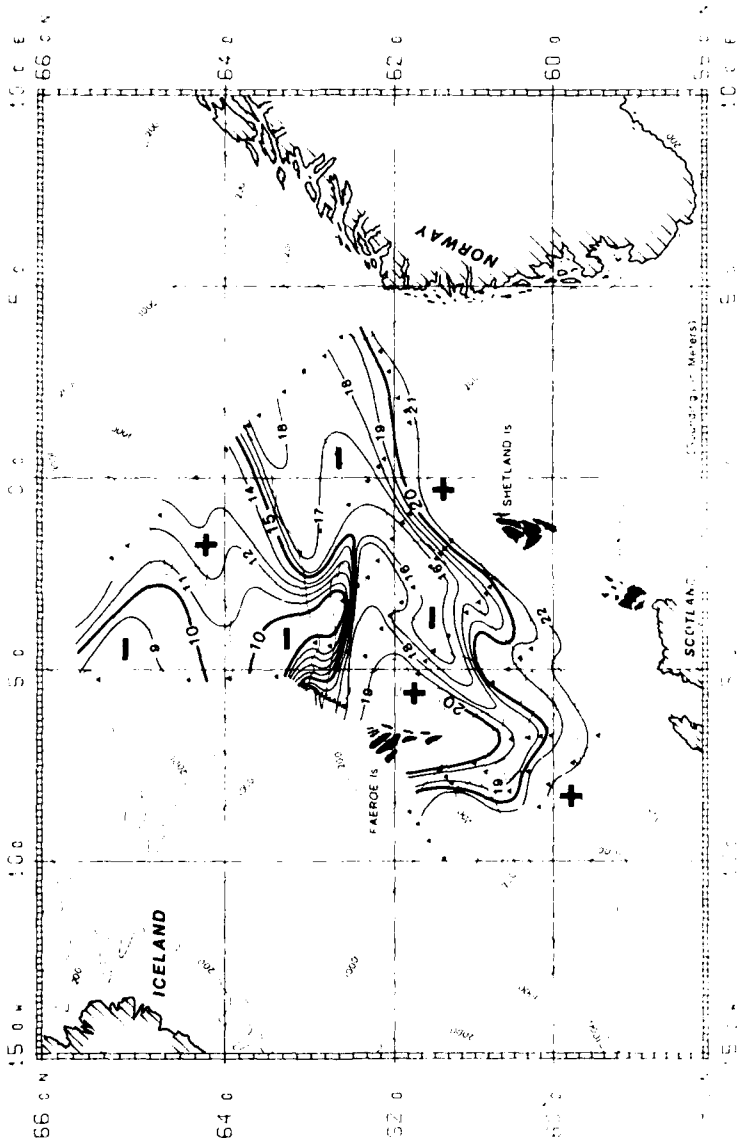

Fig. 9a. Contours of dynamic height [illegible] to 300 dbar in dynamic cm. The values are derived from the CTD stations [illegible]

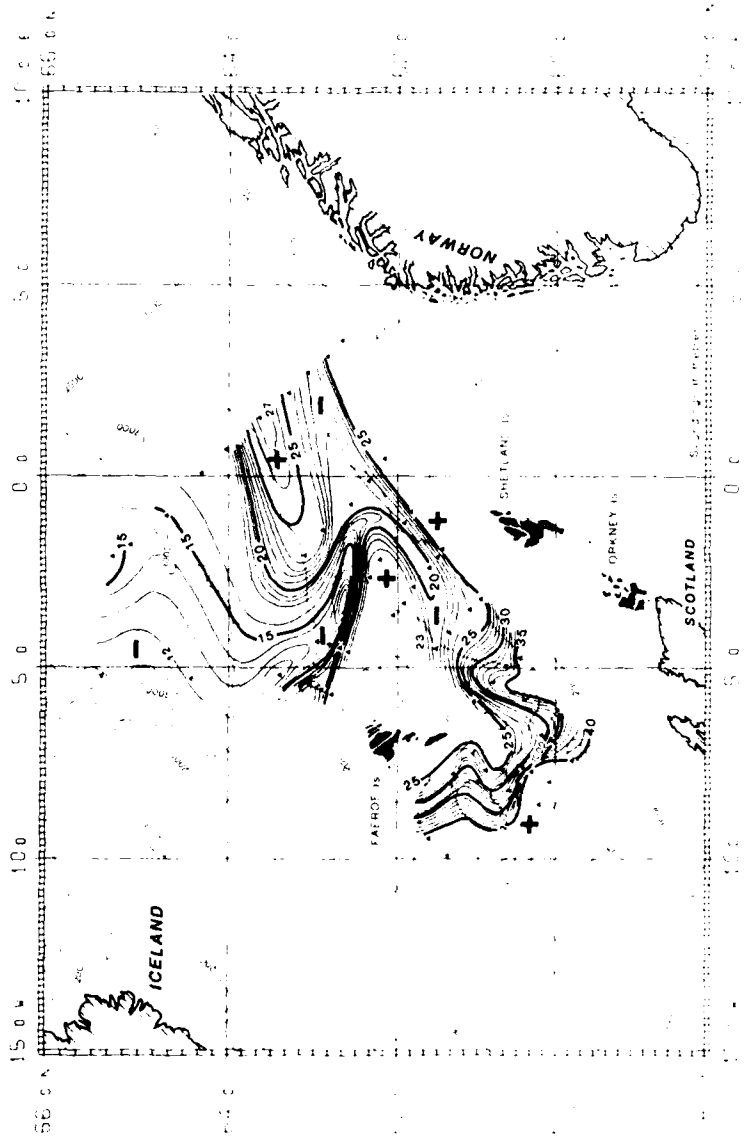

Fig. 9b As Fig. 9a, but for the layers 0 to 600 dbar.

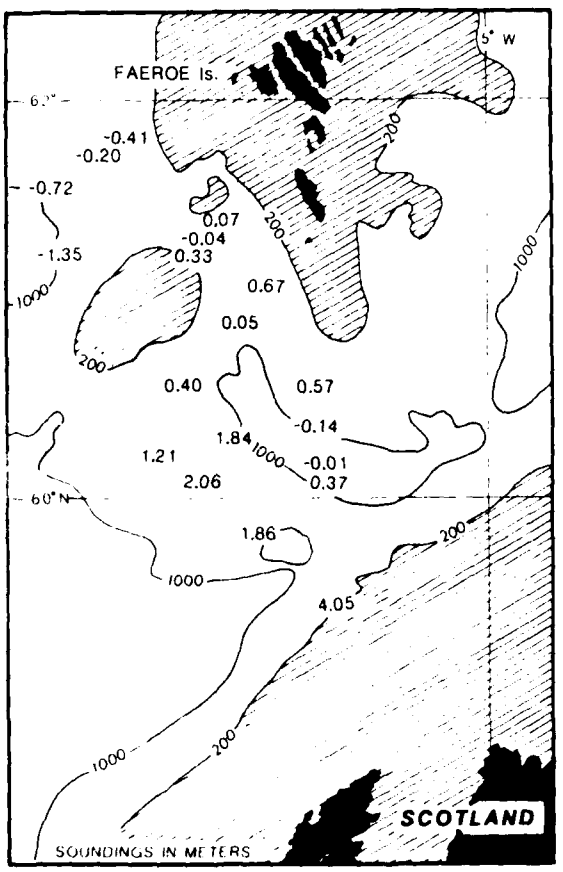

Fig. 10. Spatial distribution of errors in predicted dynamic height δ^*, derived from the measured temperature profiles to $P = 300$ dbar using the seasonal model (Table 3) and compared with those calculated from the measured profiles of temperature and conductivity. Only stations to the southwest of the Faeroe Islands, close to the COMPASS arc, have been used. The mean error is 0.56 dynamic cm, with standard deviation of 1.22 dynamic cm. The extreme values are −1.35 and 4.05 dynamic cm.

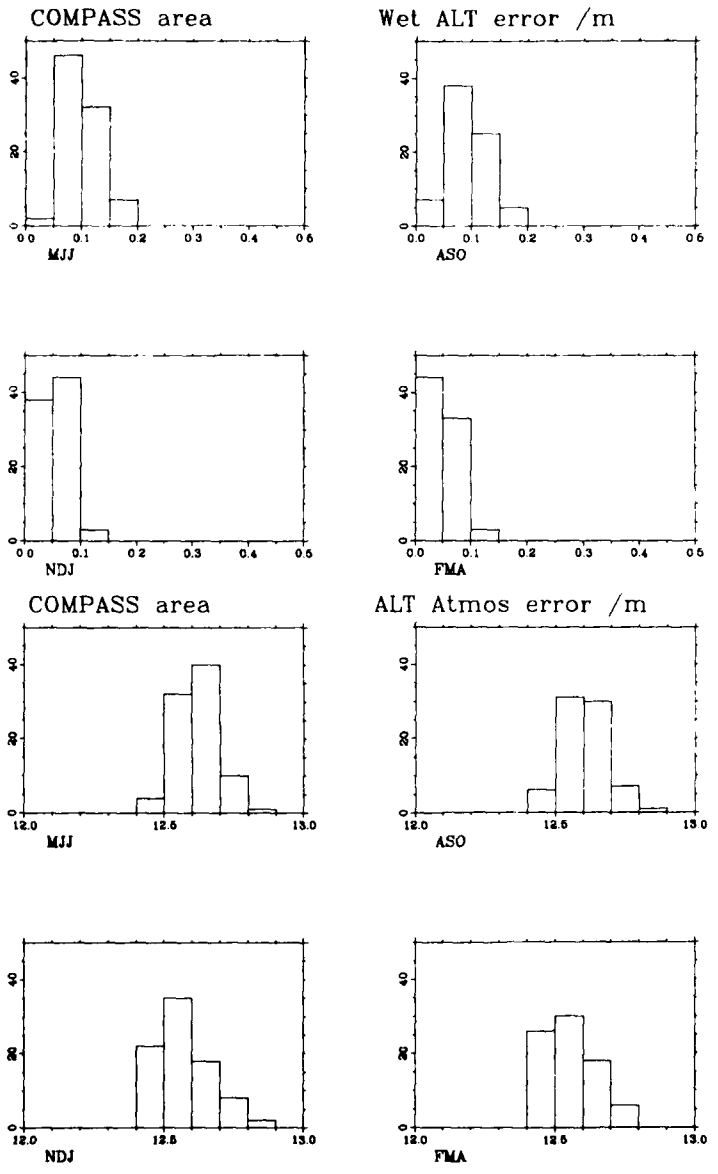

Fig. 11: Histograms of the satellite altimeter range errors caused by atmospheric variability. Those caused by the wet tropospheric effect are shown above the total errors. The values were derived from radiosonde ascents close to the COMPASS arc, and are grouped into seasons (May–Jul; Aug–Oct; Nov–Jan; Feb–Apr).

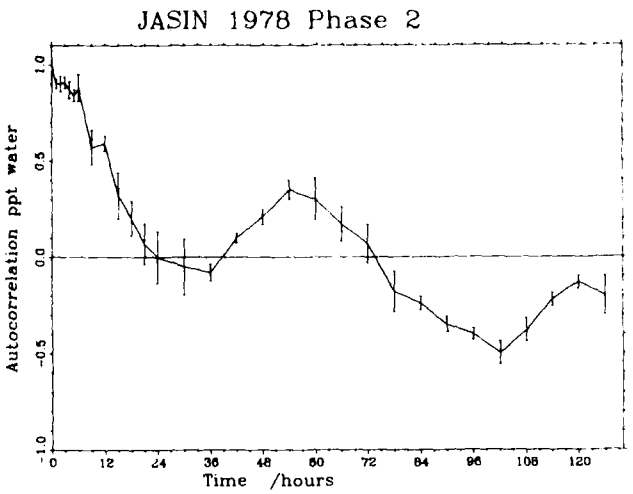

Fig. 12: The autocorrelation function for precipitable water (w) measured from ships in the summer/autumn of 1978 during the JASIN experiment. [After Taylor, 1983.]

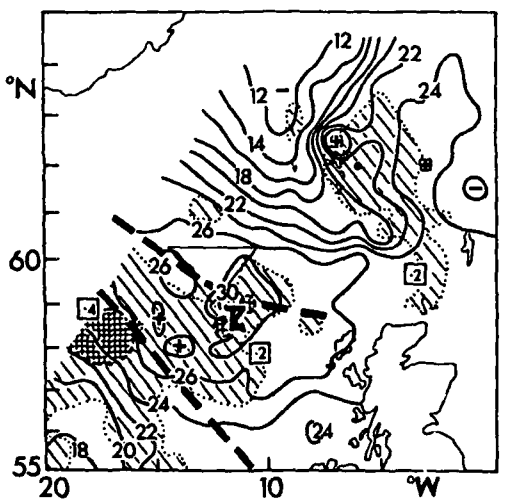

Fig. 13: Contours of precipitable water ($kg\,m^{-2}$) and the distribution of liquid water ($kg\,m^{-2}$), shaded areas with values in boxes, for 2134GMT 4 August 1978. The thunderstorm symbol marks the region of deep convective activity. The data are from the SEASAT SMMR (Scanning Multichannel Microwave Radiometer). The local maximum close to the Faeroe Islands is probably erroneous being caused by the presence of land. (From Taylor, Guymer, Katsaros and Lipes, 1983).

Initial Distribution for SR-128

Ministries of Defence	
JSPHQ Belgium	2
DND Canada	10
CHOD Denmark	8
MOD France	8
MOD Germany	15
MOD Greece	11
MOD Italy	10
MOD Netherlands	12
CHOD Norway	10
MOD Portugal	2
MOD Spain	2
MOD Turkey	5
MOD UK	20
SECDEF US	68
NATO Authorities	
Defence Planning Committee	3
NAMILCOM	2
SACLANT	10
SACLANTREPEUR	1
CINCWESTLANT/ COMOCEANLANT	1
COMSTRIKFLTANT	1
CINCIBERLANT	1
CINCEASTLANT	1
COMSUBACLANT	1
COMMAIREASTLANT	1
SACEUR	2
CINCNORTH	1
CINCSOUTH	1
COMNAVSOUTH	1
COMSTRIKFORSOUTH	1
COMEDCENT	1
COMMARAIRMED	1
CINCHAN	3
SCNR for SACLANTCEN	
SCNR Belgium	1
SCNR Canada	1
SCNR Denmark	1
SCNR Germany	1
SCNR Greece	1
SCNR Italy	1
SCNR Netherlands	1
SCNR Norway	1
SCNR Portugal	1
SCNR Turkey	1
SCNR UK	1
SCNR US	2
French Delegate	1
SECGEN Rep. SCNR	1
NAMILCOM Rep. SCNR	1
National Liaison Officers	
NLO Canada	1
NLO Denmark	1
NLO Germany	1
NLO Italy	1
NLO UK	1
NLO US	1
NLR to SACLANT	
NLR Belgium	1
NLR Canada	1
NLR Denmark	1
NLR Germany	1
NLR Greece	1
NLR Italy	1
NLR Netherlands	1
NLR Norway	1
NLR Portugal	1
NLR Turkey	1
NLR UK	1
Total external distribution	257
SACLANTCEN Library	10
Stock	13
Total number of copies	280

END

DATE

FILMED

3 88